

In vivo ^{13}C NMR spectroscopy and metabolic modeling in the brain: a practical perspective

Pierre-Gilles Henry*, Gregor Adriany, Dinesh Deelchand, Rolf Gruetter, Malgorzata Marjanska,
Gülin Öz, Elizabeth R. Seaquist, Alexander Shestov, Kâmil Uğurbil

Center for Magnetic Resonance Research, University of Minnesota, Minneapolis, MN 55455, USA

Received 21 November 2005; accepted 21 November 2005

Abstract

In vivo ^{13}C NMR spectroscopy has the unique capability to measure metabolic fluxes noninvasively in the brain. Quantitative measurements of metabolic fluxes require analysis of the ^{13}C labeling time courses obtained experimentally with a metabolic model. The present work reviews the ingredients necessary for a dynamic metabolic modeling study, with particular emphasis on practical issues. © 2006 Elsevier Inc. All rights reserved.

Keywords: ^{13}C NMR spectroscopy; Metabolic modeling; TCA cycle; Glutamatergic neurotransmission; Compartmentation

1. Introduction

Carbon-13 NMR spectroscopy is a powerful tool to investigate intermediary metabolism. The high chemical specificity of ^{13}C NMR, which can distinguish ^{13}C isotope incorporation not only into different molecules, but also into specific carbon positions within the same molecule (^{13}C isotopomers), allows one to follow the fate of ^{13}C label through multiple metabolic pathways. However, the interpretation of ^{13}C NMR data to derive quantitative metabolic fluxes requires analysis with a metabolic model. This metabolic modeling is particularly complex in the brain due to the highly organized interaction between different cell types corresponding to different metabolic compartments.

The potential of ^{13}C NMR spectroscopy to study metabolic pathways was demonstrated using suspensions of microorganisms [1,2]. The first attempt to model the flow of ^{13}C label into the TCA cycle was made in 1983 by Chance et al. [3] in the heart, at a time when such analysis required some of the fastest computers available. Initial studies in the brain in vivo were reported in the late 1980s and early 1990s [4–7]. Since then, the steady increase in magnetic fields available for in vivo studies and progress in NMR methodology have allowed detection of ^{13}C labeling time courses in localized regions of the brain with constantly improving sensitivity. In parallel, methods for

metabolic modeling have evolved from relatively simple models into complex two-compartment models. Together, these improvements have allowed ^{13}C metabolic modeling studies to make important contributions to our understanding of brain metabolism and compartmentation, showing for example that the glutamate–glutamine cycle is a major metabolic pathway in the brain [8,9], that the neuronal TCA cycle rate increases with neuronal activity [10–12], that glial TCA cycle is significant in the brain [13] and that anaplerotic pyruvate carboxylase activity is significant in the brain [13] and increases with neuronal activity [14].

The aim of this review is to provide the reader with an overview of the experimental design for a ^{13}C metabolic modeling study. This is not intended as a comprehensive review of the field of ^{13}C metabolic modeling, but rather as a practical guide for readers (not only NMR spectroscopists, but also neuroscientists in general) interested in understanding the experimental details of such studies. The emphasis has been placed on metabolic modeling rather than NMR spectroscopy, and NMR spectroscopy methodology is described only when it is relevant to metabolic modeling. We refer the reader to recent reviews for further details on NMR methodology [15,16].

We have chosen to focus in this review on metabolic modeling which uses a one-compartment model and [$1\text{-}^{13}\text{C}$]glucose or [$1,6\text{-}^{13}\text{C}_2$]glucose as a metabolic substrate. Other tracers and more complex metabolic models can be used, such as two-compartment (neuron–astrocyte) models.

* Corresponding author. Tel.: +1 612 626 2001; fax: +1 612 626 2004.
E-mail address: henry@cmrr.umn.edu (P.-G. Henry).

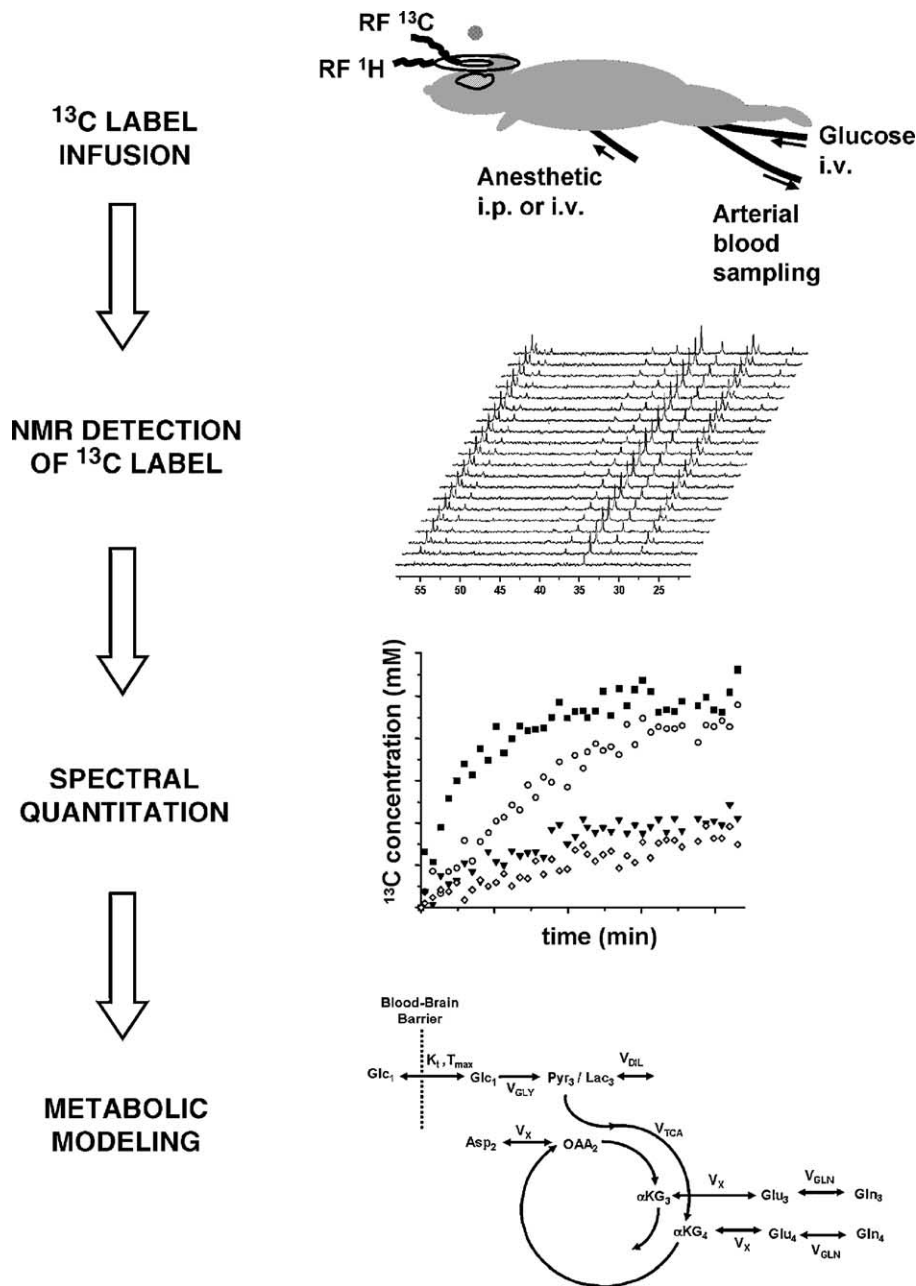


Fig. 1. Overview of a ^{13}C metabolic modeling study.

However the one-compartment model is relatively simple and is well suited for explaining the principles of metabolic modeling. We have also chosen to focus on “dynamic” metabolic modeling, meaning modeling of ^{13}C labeling time courses. Therefore other analysis methods such as isotope analysis will not be considered in this review.

^{13}C metabolic studies commonly involve four steps (Fig. 1):

- (1) choice of ^{13}C -labeled substrate and infusion protocol
- (2) detection of ^{13}C label incorporation into brain metabolites during infusion of ^{13}C labeled substrate
- (3) quantitation of ^{13}C spectra to obtain ^{13}C turnover curves

- (4) metabolic modeling of ^{13}C turnover curves to obtain quantitative fluxes through specific biochemical pathways

In the following sections, each of these steps will be examined separately, with a focus on the relevance of each aspect to metabolic modeling.

2. Choice of ^{13}C -labeled substrate and infusion protocol

2.1. Choice of ^{13}C -labeled substrate

The first step in the design of a ^{13}C metabolic study is the choice of a metabolic substrate. Since glucose is the main

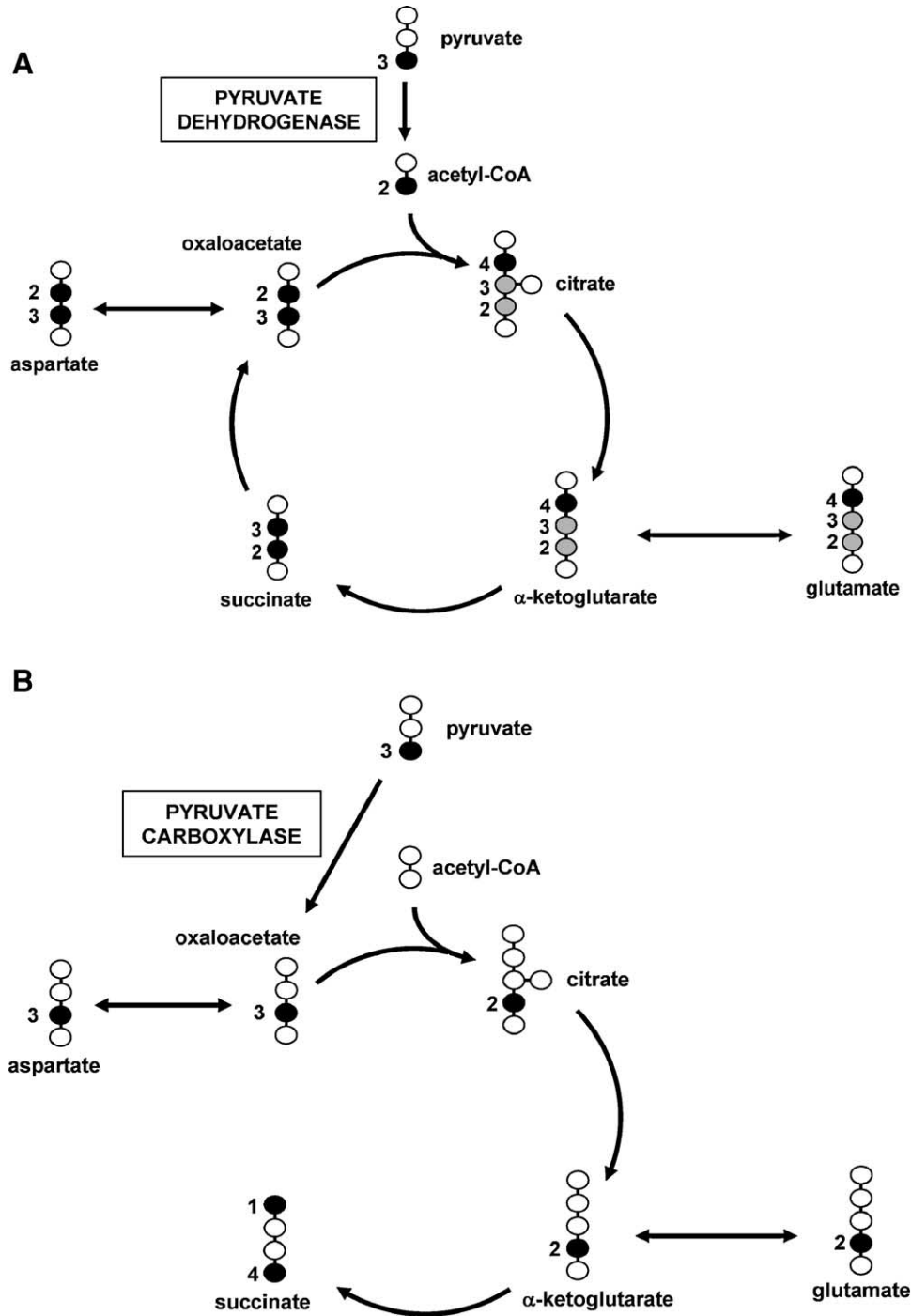


Fig. 2. ^{13}C flow from $[1-^{13}\text{C}]$ glucose into brain metabolites. (A) ^{13}C label flowing through pyruvate dehydrogenase labels the C4 of glutamate in the first turn of the TCA cycle and the C3 and C2 of glutamate in the second turn. (B) ^{13}C label flowing through pyruvate carboxylase labels the C2 of glutamate, but not the C3, leading to differential labeling of C2 and C3 positions of glutamate. See text for details.

fuel for the brain, ^{13}C -labeled glucose has been the preferred substrate for metabolic studies in the brain. Most in vivo metabolic studies have been performed using $[1-^{13}\text{C}]$ glucose or $[1,6-^{13}\text{C}_2]$ glucose. Both substrates lead to the formation of $[3-^{13}\text{C}]$ pyruvate, with $[1-^{13}\text{C}]$ glucose generating one unlabeled pyruvate and one labeled pyruvate per molecule of glucose, while $[1,6-^{13}\text{C}_2]$ glucose generates two molecules of $[3-^{13}\text{C}]$ pyruvate per molecule of glucose.

Knowledge of metabolic pathways through which the infused ^{13}C -labeled substrate can be metabolized is, of course, essential for the interpretation of ^{13}C NMR data. The flow of ^{13}C label from $[1-^{13}\text{C}]$ glucose or $[1,6-^{13}\text{C}_2]$ glucose into brain amino acids is shown in Fig. 2. Note that this figure does not take into account cellular compartmentation. For example, the enzyme pyruvate carboxylase is localized exclusively in astrocytes. See Section 4.6 for further

discussion of metabolic modeling using two-compartment models.

Through glycolysis, $[1-^{13}\text{C}]$ glucose (or $[1,6-^{13}\text{C}_2]$ glucose) generates $[3-^{13}\text{C}]$ pyruvate. Pyruvate can then be metabolized either through pyruvate dehydrogenase (Fig. 2A) or pyruvate carboxylase (Fig. 2B).

Through pyruvate dehydrogenase (Fig. 2A), $[3-^{13}\text{C}]$ pyruvate yields $[2-^{13}\text{C}]$ acetyl-CoA, which then combines with an unlabeled molecule of oxaloacetate to generate citrate labeled at the C4 position. Subsequently, α -ketoglutarate (also called 2-oxoglutarate) becomes labeled at the C4 position. The large pool of cytosolic glutamate then becomes labeled at the C4 position through transamination of $[4-^{13}\text{C}]\alpha$ -ketoglutarate and transport through the mitochondrial membrane. ^{13}C -label then goes on to label glutamine and GABA. At the same time, ^{13}C label continues to flow into the TCA cycle, labeling succinate. Since succinate is a symmetric molecule, the C2 and C3 positions of succinate cannot be distinguished and become labeled with equal probability. The first turn of the TCA cycle is completed when oxaloacetate becomes labeled at the C2 and C3 positions, eventually leading to labeling of aspartate at the C2 and C3 positions. Labeled molecules of oxaloacetate can combine again with labeled (or unlabeled) acetyl-CoA and will label the C2 and C3 positions of glutamate in the second turn of the TCA cycle.

The alternate pathway through pyruvate carboxylase (Fig. 2B) generates $[3-^{13}\text{C}]\text{oxaloacetate}$ from $[3-^{13}\text{C}]$ pyruvate. $[3-^{13}\text{C}]\text{Oxaloacetate}$ then yields $[2-^{13}\text{C}]\text{citrate}$, $[2-^{13}\text{C}]\alpha$ -ketoglutarate and $[2-^{13}\text{C}]\text{glutamate}$. Since the pyruvate carboxylase pathway labels glutamate C2, but not glutamate C3, it introduces differential labeling of glutamate at the C3 and C2 positions.

Most of the molecules that become labeled during a $[1-^{13}\text{C}]$ glucose infusion cannot be detected by NMR *in vivo* due to their low concentration and the relatively low sensitivity of *in vivo* NMR. Only the more concentrated amino acids glutamate, glutamine, aspartate and (if sensitivity is sufficient) GABA can be detected. These amino acids are not part of the TCA cycle, but reflect TCA cycle activity because they get labeled from TCA cycle intermediates α -ketoglutarate and oxaloacetate.

Although most *in vivo* ^{13}C metabolic modeling studies have used $[1-^{13}\text{C}]$ glucose or $[1,6-^{13}\text{C}_2]$ glucose infusions, other substrates have been used, e.g., $[2-^{13}\text{C}]$ glucose [17], $[1,2-^{13}\text{C}_2]$ acetate or $[2-^{13}\text{C}]$ acetate [18,19], or $[2,4]$ β -hydroxybutyrate [20]. Modeling with nonglucose substrates is complicated by the fact that, in contrast to glucose, the rate of uptake of ^{13}C -label into brain metabolism is dependent on the substrate concentration in the blood.

2.2. Infusion protocol

The infusion protocol determines the time courses of concentration and isotopic enrichment in the blood. For *in vivo* studies, the infusion protocol is usually designed to

reach a high isotopic enrichment in order to attain sufficient sensitivity for NMR detection.

Knowledge of the time course of substrate concentration and isotopic enrichment, or “input function”, is critical for deriving quantitative information from ^{13}C labeling time courses. Without knowledge of the input function, the rate of labeling of, e.g., glutamate, cannot be interpreted since one does not know how quickly the ^{13}C -labeled substrate entered the system. This input function depends on the protocol used to administer the substrate and on how quickly the substrate is metabolized. Therefore the infusion protocol must be adapted for the specific metabolic conditions under investigation.

An example of infusion protocol often used for metabolic studies is the hyperglycemic clamp. In this protocol, plasma glucose concentration is rapidly raised from euglycemic levels to hyperglycemic levels using a bolus of 99%-enriched $[1-^{13}\text{C}]$ glucose. This bolus mixes with the endogenous ^{12}C -glucose in the blood and typically yields about 70% enrichment in plasma glucose within a few minutes. The bolus is followed by a continuous infusion of 70%-enriched $[1-^{13}\text{C}]$ glucose to keep glucose concentration stable at two to three times the euglycemia levels. This protocol results in an input function that is close to a step function, reaching 70% enrichment within a few minutes and remaining at 70% isotopic enrichment thereafter.

However, the time course of plasma glucose isotopic enrichment does not need to be a step function as long as it is measured experimentally. For example, glucose can be administered orally [21,22] and the input function can be measured using blood samples taken from the subject throughout the experiment and analyzed for glucose concentration and isotopic enrichment. Alternatively, when blood cannot be drawn easily inside the magnet, as is the case for small animals (e.g., mice) with a small blood volume, additional measurements can be performed on the bench using the same infusion protocol as *in vivo* to determine the input function.

The use of glucose as a substrate presents a number of advantages for metabolic modeling in the brain. First, it is generally accepted that brain metabolism is not affected by glucose concentrations [23], as long as those remain above a certain threshold. Second, under hyperglycemic conditions, the liver releases little glucose into the blood, preventing additional sources of labeled substrates to enter the brain through the circulation.

3. Detection and quantification of ^{13}C label. What can be measured from NMR spectra *in vivo*?

The next step in the design of a ^{13}C metabolic study is the detection of ^{13}C label incorporation into brain metabolites during infusion of the ^{13}C -labeled substrates and the quantification of the resulting NMR spectra. Since most TCA cycle intermediates are not concentrated enough to be

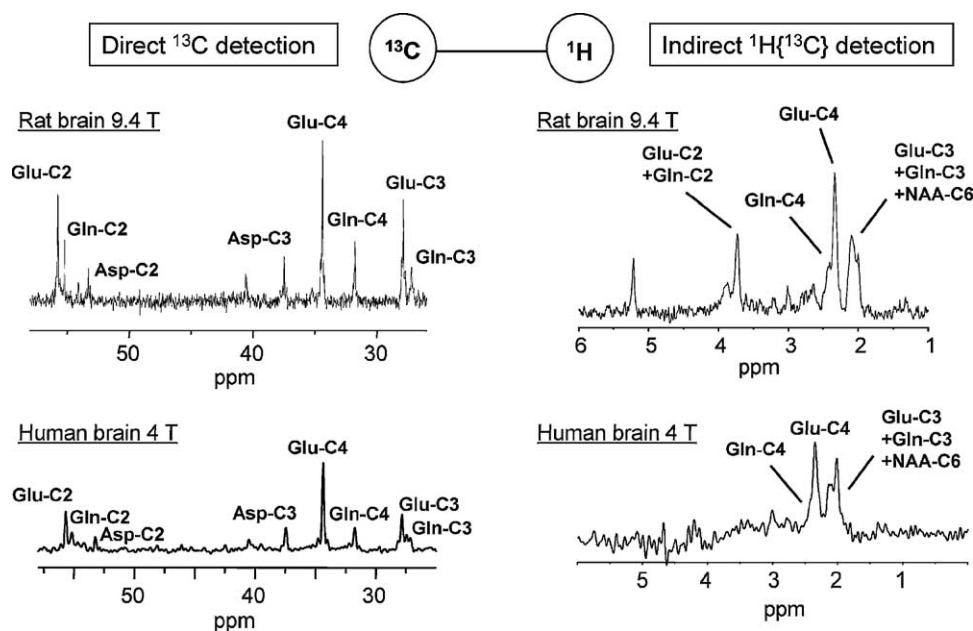


Fig. 3. In vivo localized experimental spectra obtained after ^{13}C -labeled glucose infusion in the rat brain at 9.4 T (top row) and in the human brain at 4 T (bottom row) using direct detection (left column) and indirect detection (right column). Direct detection spectra were obtained using polarization transfer [24,25] and indirect detection spectra were obtained using ^{13}C -LASER [26]. Direct detection allowed resolved detection of C4, C3, C2 resonances of glutamate and glutamine and C3, C2 carbon positions of aspartate. Indirect detection gave better sensitivity (the volume of interest was smaller), but spectral overlap prevented resolved detection of each individual carbon position. Note the high NAA C6 peak in the human ^{13}C -LASER spectrum (bottom right) due to the fact that this spectrum was acquired after a very long infusion time.

detected by NMR in vivo, one relies on detection of ^{13}C label in the larger pools of brain amino acids such as glutamate, glutamine, aspartate and (if sensitivity is sufficient) GABA.

A fundamental choice in the design of in vivo ^{13}C experiments is the choice of a method for detection of ^{13}C label. Detection methods can be broadly classified into two groups: direct detection at ^{13}C frequency and indirect detection at ^1H frequency. The choice of detection method is important because it determines what experimental data will be obtainable for metabolic modeling, which places constraints on how complex a metabolic model can be used.

The choice of the detection method is closely related to the choice of the model used for metabolic modeling. This is because the choice of the detection method determines what experimental data can be obtained from NMR spectra, such as which carbon positions can be measured in which amino acid. What can be measured in vivo is limited both by the signal-to-noise of NMR spectra and by the spectral resolution. The signal-to-noise limits detection to those compounds that have relatively high concentration and reach a high isotopic enrichment during the ^{13}C infusion. Spectral overlap, especially with indirect detection, may prevent quantification of individual resonances corresponding to distinct carbon positions.

In vivo ^{13}C NMR spectroscopy is technically challenging. Excellent reviews of the technical challenges for both direct and indirect detection have recently been published [15,16] and we only summarize them here. The main limitation of the technique is undoubtedly its low sensitivity,

and optimizing sensitivity in turn places strong demands on RF coil design and pulse sequence development. In particular, the application of decoupling during acquisition to improve signal-to-noise and reduce spectral overlap places constraints on the experimental design to minimize power deposition (especially in humans) and minimize RF interference between ^1H and ^{13}C channels. Other aspects of NMR methodology include localization and reduction of chemical-shift displacement errors.

Time courses of ^{13}C label incorporation can also be obtained in animals from brain extracts, with the disadvantage that each time point results from several different animals (cross-sectional measurement) and that measurements may be affected by postmortem changes and extraction procedures. However, such extracts studies have allowed studies of brain metabolism in the conscious rat, whereas in vivo studies require anesthesia to minimize stress and movement in the magnet. The main advantage of in vivo detection is to permit measurements of entire ^{13}C labeling time courses in a single animal, reducing the number of animals and reducing noise caused by inter-animal variability. In vivo detection, of course, also makes it possible to perform noninvasive measurements in humans.

3.1. Direct detection vs. indirect detection of ^{13}C label

Examples of recent spectra obtained with direct and indirect detection during an infusion of ^{13}C -labeled glucose are shown in Fig. 3. These show incorporation of ^{13}C label mostly into amino acids glutamate and glutamine, and with lower sensitivity aspartate and GABA. Smaller signals from

NAA and *myo*-inositol are also detected. These spectra illustrate the quandary that the scientist faces when choosing a detection method. The relative advantages and disadvantages of each method are discussed below.

3.2. Direct detection

The first studies using direct detection in the brain *in vivo* were performed by Behar et al. [5] in animals and by Beckmann et al. [27] and Gruetter et al. [7,24,28] in humans.

The main advantage of direct ^{13}C detection lies in the very high chemical specificity of ^{13}C spectroscopy due to the broad chemical shift range (~200 ppm). This has allowed resolved and simultaneous detection of C4, C3 and C2 resonances of glutamate and glutamine in both humans [29] and animals [25]. This, in turn, allows additional data to be used in the metabolic modeling, making the fitting procedure more reliable.

Another advantage of direct ^{13}C detection lies in the additional information from isotopomers. Molecules labeled at several carbon positions simultaneously appear in ^{13}C spectra as multiplets, whereas molecules labeled at only one carbon position appear as singlets. Recent progress in NMR spectroscopy has allowed detection of these isotopomers and quantification of these isotopomers *in vivo* [30]. This information can be used to calculate the isotopic enrichment at different carbon positions. For example, the doublet of glutamate at the C4 position corresponds to $[3,4\text{-}^{13}\text{C}_2]\text{glutamate}$ and directly reflects enrichment of glutamate at the C3 position.

In spite of these advantages (high chemical specificity and additional information from multiplets corresponding to different isotopomers), direct detection suffers from its relatively low sensitivity, due to the low gyromagnetic ratio of ^{13}C . Sensitivity has been improved by the use of higher field magnets and methodological improvements in NMR spectroscopy such as RF coils, shimming and new pulse sequence developments (see Ref. [15] for more details).

3.3. Indirect detection

In contrast to direct ^{13}C detection, indirect $^1\text{H}[^{13}\text{C}]$ detection (i.e., detection of ^{13}C label through the attached protons) offers better sensitivity due to the fourfold higher gyromagnetic ratio of ^1H compared to ^{13}C . The first studies using indirect detection of ^{13}C label in the brain *in vivo* were performed by Rothman et al. [4,31].

This gain in sensitivity is offset by a loss in chemical specificity due to the smaller chemical shift range of ^1H . This spectral overlap reduces the number of carbon positions that can be measured using indirect detection and reduces the amount of experimental data available for metabolic modeling.

Since spectral overlap decreases at higher magnetic field, more information can be gained at higher field. For example, separate detection of glutamate C4 and glutamine C4 (or more precisely detection of signals from protons

attached to glutamate C4 and glutamine C4) has not been possible so far in $^1\text{H}[^{13}\text{C}]$ spectra in humans even at 4 T due to spectral overlap between these two resonances. Due to the fact that the glutamine ^{13}C labeling time course is needed to exploit two-compartment models, the inability to resolve glutamate and glutamine has so far prevented measurement of glutamate–glutamine cycling in humans using indirect detection. In humans at 3 or 4 T, most indirect detection studies have measured glutamate C4 only [11,31,32], but not glutamine (neglecting contamination of the glutamate signal by glutamine). The use of higher magnetic fields (7 or 9.4 T in humans) or the use of new pulse sequences such as semiselective Proton-Observed Carbon-Edited may allow separate detection of glutamate C4 and glutamine C4 in humans in the future [33].

In studies in small animals (e.g., rat brain at 9.4 T), for which higher magnetic fields are available, glutamate C4 and glutamine C4 still show some overlap, but the two resonances can be measured relatively easily using spectral fitting routines. This is facilitated by the fact that the ratio glutamine/glutamate is higher in rats than in humans. However, separate quantitation of glutamate C3 and glutamine C3 remains difficult, due to spectral overlap between three resonances around 2.1 ppm: GluC3, GlnC3 and NAAC6. The NAAC6 resonance gets labeled more slowly than GluC3 and GlnC3. If the ^{13}C infusion time remains short, NAAC6 can be eliminated by subtracting a natural abundance spectrum acquired before the beginning of the ^{13}C infusion, and subsequent labeling of NAAC6 is neglected. Separate quantitation of glutamate C3 and glutamine C3 has been shown to be feasible at 9.4 T using LCModel [34,35]. However, a high cross-correlation between GluC3 and GlnC3 remains inevitable, and the use of GlxC3 (i.e., GluC3+GlnC3) as a single time course in the modeling analysis is preferable.

A complication for indirect detection, as pointed out in recent reports, is the potential bias in NMR quantitation introduced by strong coupling [36,37]. When strong coupling is present, the signal at a specific proton chemical shift may not directly reflect isotopic enrichment of the attached carbon.

To summarize, direct detection currently allows detection of time courses for many carbon positions (C4, C3, C2 of glutamate and glutamine, and C3, C2 of aspartate). Indirect detection currently provides more limited biochemical information (GluC4 and GluC3 in humans at 4 T, or GluC4, GlnC4 and GlxC3 in animals at 9.4 T) with higher sensitivity.

4. Metabolic modeling

The fourth and final step in a ^{13}C metabolic study is the analysis of ^{13}C labeling time courses with a metabolic model to derive quantitative metabolic fluxes. Time courses of ^{13}C labeling obtained after measurement and quantitation

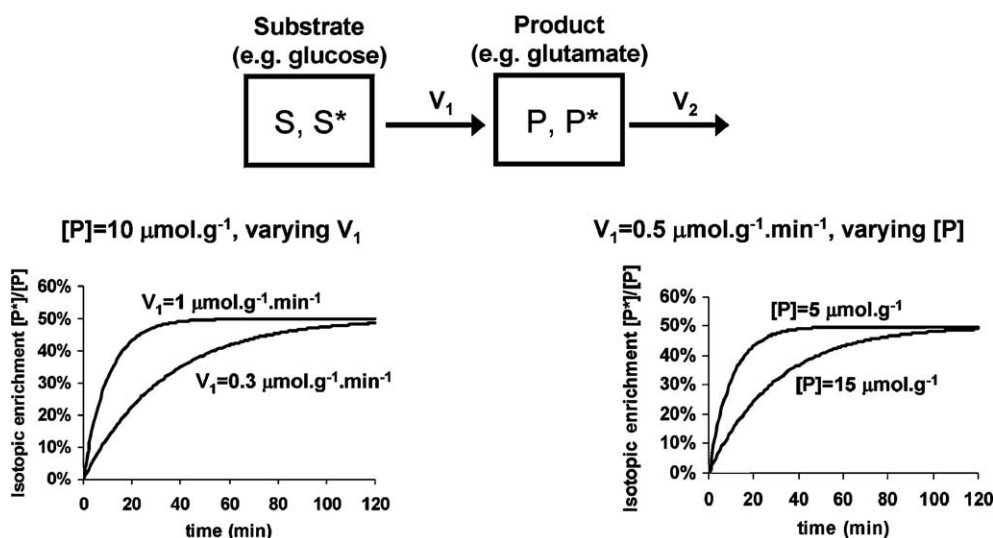


Fig. 4. Single pool model. $[S]$ and $[P]$ denote the total concentration of substrate and product, respectively. $[S^*]$ and $[P^*]$ denote the concentration of labeled substrate and labeled product, respectively. $[S^*]/[S]$ and $[P^*]/[P]$ are the isotopic enrichment of substrate and product, respectively. Labeling curves of product are shown following a step-function increase in substrate isotopic enrichment from natural abundance to 50% at $t=0$. The isotopic enrichment of the product increases exponentially to reach the isotopic enrichment of the substrate (isotopic steady-state). The rate of labeling of the product depends not only on the influx of substrate but also on the size of the product pool.

of ^{13}C NMR spectra offer only limited metabolic information unless they are further analyzed using a metabolic model. For example, the rate of labeling of glutamate C4 depends not only on the TCA cycle rate (V_{TCA}), but also on the exchange rate between α -ketoglutarate and glutamate (V_X) and on total glutamate concentration. Therefore a change in glutamate labeling time course does not necessarily reflect a change in V_{TCA} .

Metabolic modeling of dynamic ^{13}C labeling time courses allows for quantitative determination of metabolic fluxes through specific metabolic pathways. The field of metabolic modeling is still evolving, with metabolic models being refined as further experimental data become available.

4.1. Choice of a metabolic model

The choice of the model is guided by the following questions:

- what are the known biochemical pathways for the ^{13}C -labeled substrate?
- what experimental kinetic data are available from NMR spectra?
- what metabolic fluxes will be kept as free parameters, and what biochemical pathways will be assumed based on previous studies?

The main concern when addressing these questions is to choose a model that is both accurate (i.e., accurately reflects the flow of ^{13}C label from substrate to the measured products) and stable (i.e., does not have too many free parameters compared to the available experimental data). Therefore, the more experimental data available for use in

the model, the more complex the metabolic model used to analyze these data can be.

4.1.1. Single-pool model

The simplest model that can be used is the single-pool model depicted in Fig. 4. Although simple, this model is useful to demonstrate a few key points. Two types of equations can be written for the product pool. The first one is the mass balance equation, expressing that the variation of product concentration over time is equal to what enters the pool minus what exits the pool:

$$\frac{d[P]}{dt} = V_1 - V_2$$

When assuming metabolic steady state, then:

$$\frac{d[P]}{dt} = 0 \Rightarrow V_1 = V_2$$

The second equation is the isotope balance equation:

$$\frac{d[P^*]}{dt} = \frac{[S^*]}{[S]} V_1 - \frac{[P^*]}{[P]} V_2$$

If $[S]$, $[S^*]$, $[P]$, $[P^*]$ are all constant, then this equation can be solved analytically to yield:

$$[P^*] = [P] \frac{[S^*]}{[S]} \left(1 - e^{-\frac{V_1}{[P]} t} \right)$$

If the isotopic enrichment of the substrate $[S^*]/[S]$ is a step function, increasing from 1.1% to 50% at $t=0$ and remaining at 50% thereafter, then $[P^*]$ increases exponentially to reach a steady-state enrichment of 50% identical to

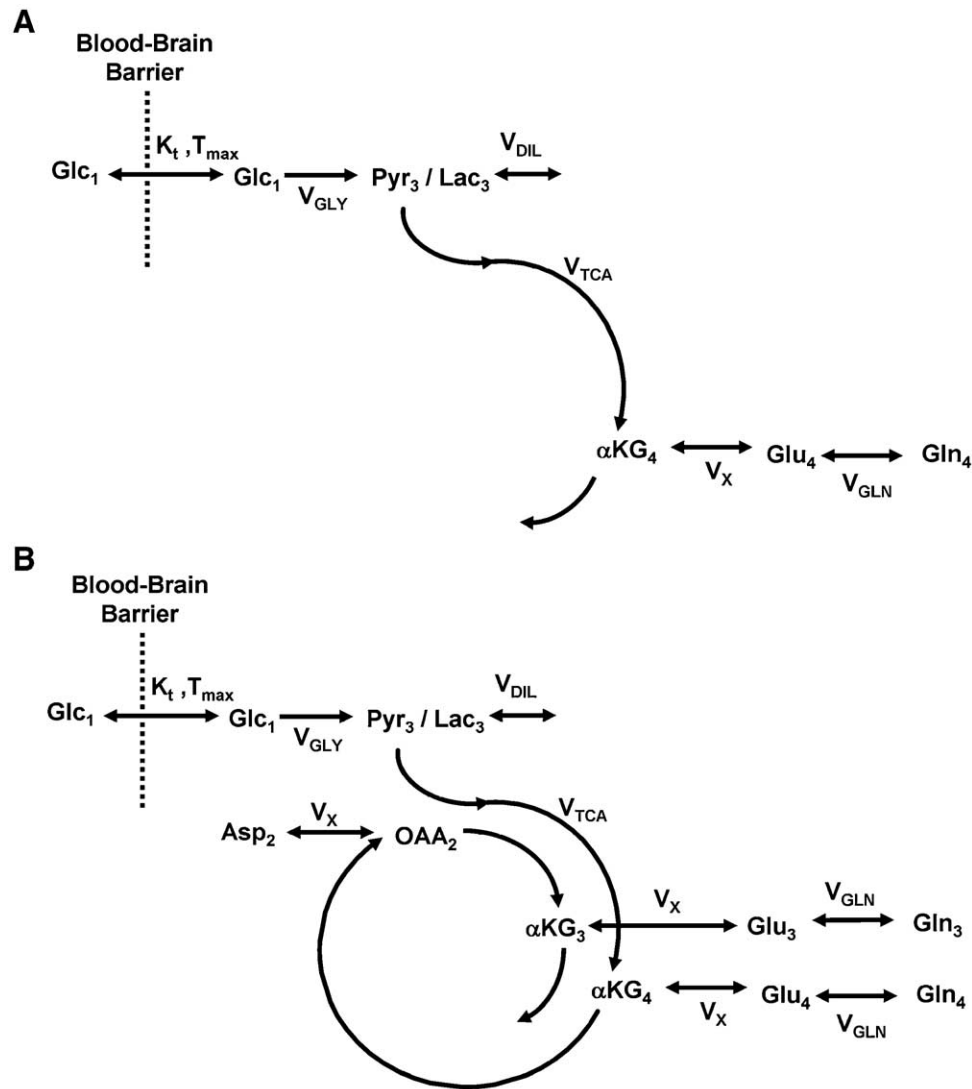


Fig. 5. One-compartment model describing the flux from $[1-^{13}\text{C}]$ glucose into glutamate. (A) Model used to analyze the glutamate C4 labeling curve after one turn of TCA cycle. (B) Model used to analyze both glutamate C4 and glutamate C3 labeling curves after two turns of TCA cycle.

that of the substrate (Fig. 4). Note that the rate of labeling of the product is dependent not only on the influx V_1 but also on the concentration of the product [P].

4.1.2. One-compartment model of brain metabolism

In most cases, the single-pool model is not sufficient to accurately measure fluxes such as V_{TCA} in the brain because the overall flux from, e.g., glucose to glutamate, comprises several different metabolic fluxes such as V_{TCA} and V_X . One model that has been often used to analyze ^{13}C turnover curves in the brain is the so-called one-compartment model. This model describes the flow of $[1-^{13}\text{C}]$ glucose either into glutamate C4 alone (Fig. 5A) or into glutamate C4 and glutamate C3 (Fig. 5B). Since most glutamate is located in neurons, fluxes obtained using this model reflect primarily neuronal metabolism.

An important consideration when choosing the metabolic model is to decide how many degrees of freedom will be

left (i.e., how many free parameters will be allowed in the fit, the other parameters being fixed based on assumptions). For the one-compartment model, up to three free parameters are typically used: the TCA cycle rate V_{TCA} , the exchange rate between α -ketoglutarate and glutamate (V_X), and the isotopic dilution rate (V_{DIL}) due to exchange of labeled lactate with unlabeled lactate. The flux from glutamate to glutamine (V_{GLN}) is often assumed based on literature values if glutamine time courses are not measured. As shall be seen later in this section, the robustness of the fit can be greatly reduced if too many degrees of freedom are allowed together with too little experimental data.

The following underlying assumptions have to be verified for the model to be valid:

- Fluxes are constant over the duration of the experiment.
- Pool sizes are constant (This is often the case, but this is not an absolute requirement. For example, brain

glucose concentration changes over time at the beginning of the glucose infusion when going from euglycemia to hyperglycemia).

- Pool sizes are known.
- Small metabolic pools can be grouped to form a single metabolic pool (e.g., the oxaloacetate pool actually represents all pools from succinate to oxaloacetate).

4.2. Mathematical expression of the model

Once the model has been defined, it is expressed mathematically in a form suitable for numerical calculations. Several programs are currently in use for metabolic modeling. Some have used direct implementation of differential equations in Matlab [38]. Other programs feature a graphic interface that allows the user to define the model graphically (e.g., SAAM, CWAVE). The program then automatically generates the equations for the numerical calculations. These programs are very convenient to use, but may sometimes be less flexible than Matlab, e.g., to perform Monte Carlo simulations.

Considering the one-compartment model in Fig. 5A, four differential equations are needed to express the model in a mathematical form, one for each pool in the model: pyruvate/lactate (considered as a single pool), α -ketoglutarate, glutamate, glutamine. These equations are obtained by writing the isotope balance equation for each pool. Mass balance equations are not needed if pool sizes are assumed to be constant. This gives a set of four differential equations. For example, the isotope balance equation for lactate is:

$$\frac{d[\text{L3}]}{dt} = V_{\text{GLY}} \cdot \frac{[\text{GLC1}]}{[\text{GLC}]} - (V_{\text{TCA}} + V_{\text{DIL}}) \cdot \frac{[\text{L3}]}{[\text{L}]}$$

This equation expresses that the variation of labeled lactate over time is equal to the amount of ^{13}C label that enters the pool coming from glucose $\left(V_{\text{GLY}} \cdot \frac{[\text{GLC1}]}{[\text{GLC}]}\right)$ minus the amount of ^{13}C label that exits the pool to the TCA cycle $\left(V_{\text{TCA}} \cdot \frac{[\text{L3}]}{[\text{L}]}\right)$ and through exchange with unlabeled lactate $\left(V_{\text{DIL}} \cdot \frac{[\text{L3}]}{[\text{L}]}\right)$. In this equation, [L3] is the concentration of lactate labeled at the C3 position and [L] is the total (and constant) concentration of lactate. Similarly, [GLC1] is the concentration of brain glucose labeled at the C1 position and [GLC] is the total brain glucose concentration (not constant in general). V_{GLY} is the rate of glycolysis and is assumed to be half of V_{TCA} because one molecule of glucose generates two molecules of pyruvate through glycolysis.

Similar equations are obtained for the three other metabolic pools:

$$\frac{d[\alpha\text{KG4}]}{dt} = V_{\text{TCA}} \cdot \frac{[\text{L3}]}{[\text{L}]} + V_{\text{X}} \cdot \frac{[\text{GLU4}]}{[\text{GLU}]} - (V_{\text{TCA}} + V_{\text{X}}) \times \frac{[\alpha\text{KG4}]}{[\alpha\text{KG}]}$$

$$\frac{d[\text{GLU4}]}{dt} = V_{\text{X}} \cdot \frac{[\alpha\text{KG4}]}{[\alpha\text{KG}]} - (V_{\text{X}} + V_{\text{GLN}}) \cdot \frac{[\text{GLU4}]}{[\text{GLU}]} + V_{\text{GLN}} \cdot \frac{[\text{GLN4}]}{[\text{GLN}]}$$

$$\frac{d[\text{GLN4}]}{dt} = V_{\text{GLN}} \cdot \left(\frac{[\text{GLU4}]}{[\text{GLU}]} - \frac{[\text{GLN4}]}{[\text{GLN}]} \right)$$

Finally, the time course of brain glucose enrichment ($[\text{GLC1}]/[\text{GLC}]$) can be obtained from the time course of plasma glucose concentration and isotopic enrichment by adding two more equations for glucose transport (one for mass balance and one for isotope balance) as in Ref. [13]. Note that the equation for mass balance is needed for glucose because brain glucose concentration does not stay constant when going from euglycemia to hyperglycemia at the beginning of the ^{13}C -glucose infusion.

4.3. Fitting procedure

The system of differential equations describing the model is in general difficult to solve analytically, but it can be solved numerically. An overview of the fitting procedure is presented in Fig. 6.

In order to fit the glutamate C4 labeling time course with the one-compartment model of Fig. 5A, for example, one starts with initial values of the free parameters V_{X} and V_{TCA} . Solving the system of differential equations gives the ^{13}C labeling time course of glutamate C4 corresponding to the initial values of V_{TCA} and V_{X} . This time course is compared with the experimentally measured GluC4 time course by calculating the fit residuals. Residuals are then minimized using a least-squares procedure such as Levenberg–Marquardt to determine the value of parameters V_{TCA} and V_{X} that give the best fit of the calculated ^{13}C labeling curve to the experimental data.

A well-recognized potential problem when performing least-square fitting is the possibility of finding a local minimum that is different from the absolute minimum. Such a nonrobust fit is more likely to happen if the problem is underdetermined (too many free parameters compared to available experimental data).

Inspection of the fit residuals indicates whether there is any systematic bias in the fit. Nonrandom residuals can point to an inaccurate model, an inaccurate input function or inaccurate quantitation of NMR data. In all cases, nonrandom residuals should alert the scientist about potential flaws in the analysis.

4.4. Evaluation of fit reliability: Monte Carlo simulations

Given the complexity of metabolic models, it is essential to make sure that the analysis is robust and that the fit is not unstable, a situation that happens typically when there are too many degrees of freedom in the model compared to the available experimental data. Estimates of the standard

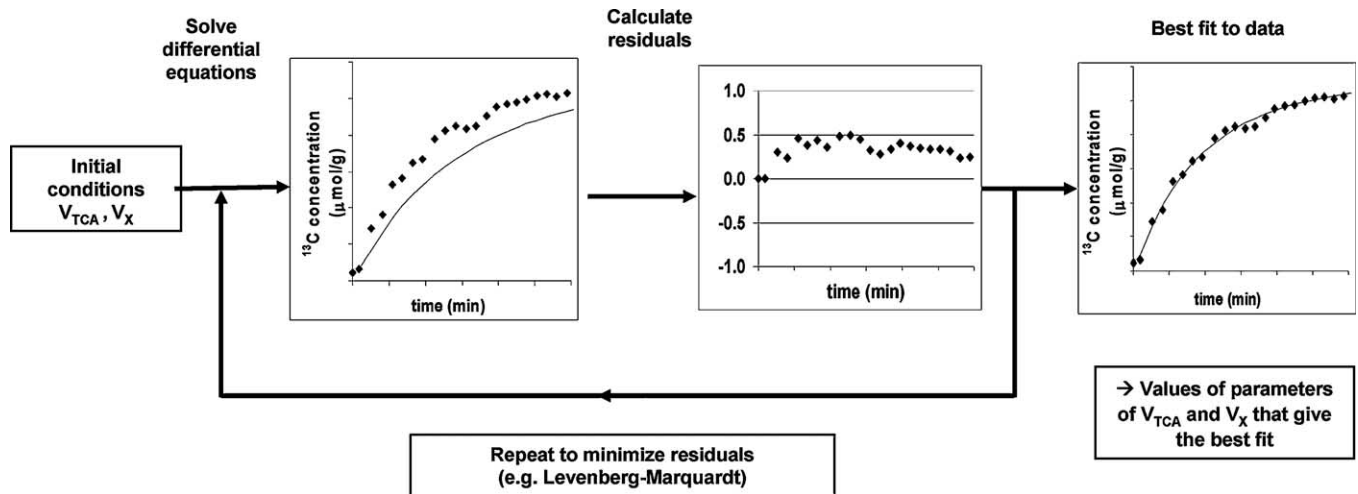


Fig. 6. Overview of fitting procedure.

deviation on fitted parameters can be obtained from the fitting algorithm, but these estimates may not be accurate especially if the noise level is high [39]. Therefore Monte Carlo simulations (i.e., repeating the same fit several hundred times with the same noise level, but a different noise realization) are the tool of choice to evaluate the robustness of the model.

An example of “underdetermined” problem occurs when fitting the glutamate C4 time course with a one-compartment model while keeping both V_{TCA} and V_X as free parameters (Fig. 7). In that case, the glutamate C4 curve is perfectly fitted, but Monte Carlo simulations show that the determination of V_{TCA} and V_X is not reliable, because V_{TCA} and V_X values are spread over a large range of values.

When an underdetermined problem like this occurs, two different solutions can be adopted.

The first option is to reduce the number of degrees of freedom in the model by constraining some of the free parameters. This can be done in the above example by fixing V_X to a specific value. However, the specific assumption on V_X can have a profound impact on the calculated V_{TCA} . For example, in a study by Henry et al. [38], it was shown that fitting the glutamate C4 time course while assuming V_X to be very fast ($V_X=50 \mu\text{mol g}^{-1} \text{min}^{-1}$) resulted in a V_{TCA} value after fitting of $0.43 \mu\text{mol g}^{-1} \text{min}^{-1}$. When V_X was constrained to $1 \mu\text{mol g}^{-1} \text{min}^{-1}$, V_{TCA} was found to be $0.66 \mu\text{mol g}^{-1} \text{min}^{-1}$, a more than 50% increase compared to the value found with $V_X=50 \mu\text{mol g}^{-1} \text{min}^{-1}$.

There is still no consensus on the value of V_X . Early studies have suggested that V_X was very fast compared to V_{TCA} [40]. Later studies have challenged this finding [13,28,38,41] and have found that V_X is comparable to

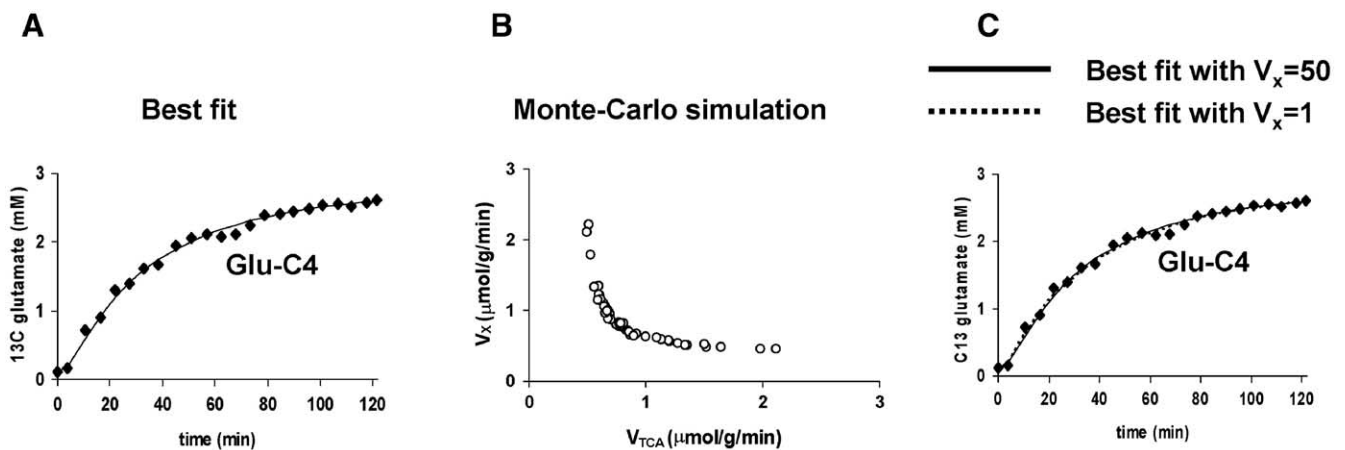


Fig. 7. Fit of glutamate C4 labeling curve with a one-compartment model. (A) Fit of glutamate C4 with two free parameters V_{TCA} and V_X . (B) Monte Carlo simulation with two free parameters V_{TCA} and V_X showing that the fit is not robust when fitting the glutamate C4 curve alone with two free parameters. (C) Effect of constraining V_X to either 50 or $1 \mu\text{mol g}^{-1} \text{min}^{-1}$. The fit is nearly identical, but the resulting value of V_{TCA} is changed by more than 50% depending on the assumption on V_X .

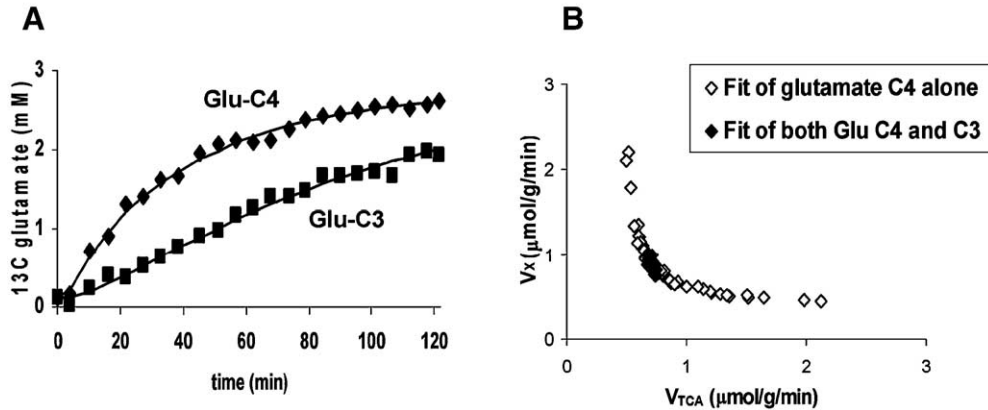


Fig. 8. Fit of both glutamate C4 and glutamate C3 labeling curves with a one-compartment model. (A) Best fit and (B) Monte Carlo simulation showing that the fit is more robust when fitting both glutamate C4 and C3 curves than when fitting the glutamate C4 curve alone.

V_{TCA} as it is in the heart [42]. This finding of low V_X is supported by measurements in isolated brain mitochondria [43] and is consistent with the fact that V_X may reflect malate–aspartate shuttle activity. Unfortunately, precise determination of V_X in ¹³C modeling studies remains hampered by the intrinsically low numerical accuracy on the determination of this particular flux.

The second option when facing an underdetermined problem is to increase the amount of experimental data in the modeling. In the case of glutamate analysis with a one-compartment model, this can be done by analyzing not only the GluC4 time course, but also the GluC3 time course (Fig. 8). In that case, Monte Carlo simulations clearly show that the modeling is more robust, leading to values of both V_{TCA} and V_X that are well determined (Fig. 8B).

4.5. Evaluation of fit reliability: sensitivity analysis

In addition to Monte Carlo simulations, the sensitivity of the modeling to the various assumptions needs to be evaluated. This can be done by modifying assumptions and determining the resulting effect on the fitted parameter values. An example of sensitivity analysis described earlier (Section 4.4) is the sensitivity of V_{TCA} (up to 50%) to an assumption on V_X when fitting only the glutamate C4 turnover curve. Note that constraining V_X when fitting both GluC4 and GluC3 time courses will not affect V_{TCA} as much as when fitting GluC4 alone, but may introduce nonrandom residuals.

When fitting multiple time courses, ¹³C time courses for different carbon positions need to be correctly scaled relative to each other. If the relative scaling is not correct (for example due to a possible bias in the quantification of NMR spectra), then the value of fitted parameters may be affected. For example, when fitting both glutamate C4 and glutamate C3, wrong scaling of the C3 curve relative to C4 will affect both V_{TCA} and V_X [38].

4.6. Two-compartment model vs. one-compartment model

In this review, we have focused primarily on the one-compartment model to measure V_{TCA} . Since glutamate is mostly neuronal, the V_{TCA} value obtained with this model reflects primarily neuronal V_{TCA} . The principles and ideas discussed in this review are directly applicable to more complex models such as two-compartment models.

Most of the recent developments in the field of metabolic modeling in the brain have used a two-compartment model that takes into account the cellular compartmentation between neurons and astrocytes (Fig. 9). In contrast to using a one-compartment model, which allows only determination of (mostly neuronal) V_{TCA} and V_X using glutamate labeling time courses, using a two-compartment model potentially allows for the measurement of many more metabolic fluxes, including the glial TCA cycle rate ($V_{TCA(G)}$), the pyruvate carboxylase flux (V_{PC}) and the glutamate–glutamine cycle (termed V_{CYCLE} or V_{NT}), which may reflect directly glutamatergic neurotransmission.

The development of two-compartment models was initiated with the studies of Sibson et al. [8,44] showing

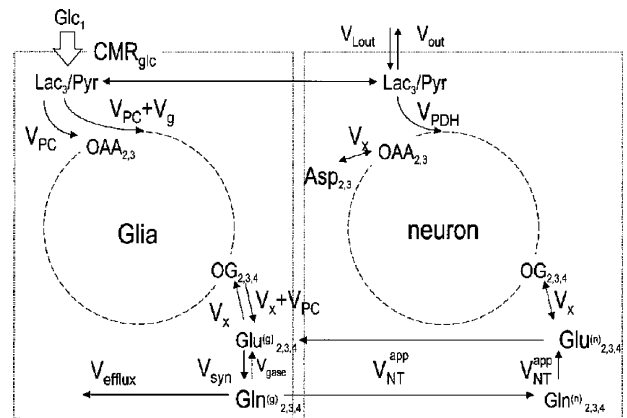


Fig. 9. Two-compartment model. Reproduced with permission from Ref. [13].

that the glutamate–glutamine cycle flux was a quantitatively significant pathway for glutamine synthesis in the brain. In these studies, the model was not fully two-compartmental, in that it did not include free parameters for the glial TCA cycle or the pyruvate carboxylase flux. The model was refined in the next few years to include a complete glial compartment with its own TCA cycle, and with pyruvate carboxylase activity in the glial compartment [13,29,45]. Some models currently in use consist of up to seven free parameters: $V_{TCA(N)}$, $V_{TCA(G)}$, V_X , V_{DIL} , V_{NT} , V_{PC} and an additional flux termed V_{EX} for isotopic dilution of ^{13}C label in glutamine through exchange with unlabeled glutamine in the blood [14]. More free parameters may even be added as models evolve. The implementation of three-compartment models (glutamatergic neurons, GABAergic neurons and astrocytes) has also been reported [46].

In spite of the complexity of two-compartment models, no systematic evaluation of their robustness has been reported so far, and more work is clearly needed in this area. Since two-compartment models are more complex than one-compartment models, it can be expected that more experimental data are needed to achieve robust modeling. For example, since differential labeling of C2 and C3 positions of glutamate and glutamine from $[1-^{13}\text{C}]\text{glucose}$ is obtained through the pyruvate carboxylase flux, information from C3 and C2 labeling time courses may be expected to provide a more reliable determination of V_{PC} .

5. Conclusion

^{13}C metabolic modeling is still an evolving field. Although this review has focused on the one-compartment model to illustrate the key points in metabolic modeling, much progress can be expected in the next few years as two-compartment models are being refined and validated. We expect Monte Carlo simulations to play a key role in the assessment of the robustness of two-compartment models in a variety of experimental conditions.

With the availability of very high magnetic fields for human studies (7 and 9.4 T), decoupling will most likely become a limiting factor, and new approaches are being developed to perform ^{13}C measurements without decoupling, using either indirect detection [47,48] or direct detection [49].

Progress in the quantitation of indirect $^1\text{H}\{^{13}\text{C}\}$ spectra is also expected as the effect of strong coupling is being investigated [36,37].

The potential of ^{13}C metabolic modeling to noninvasively measure glucose oxidative metabolism in neurons and glia and glutamatergic neurotransmission provides a huge incentive to make this approach more robust and more widespread than it is now. It is our hope that this review will encourage new investigators to begin working with this fascinating tool.

Acknowledgments

We would like to thank Dee Koski for technical assistance. This work was supported in part by NIH grants P41-RR08079, R01-NS38672, the Keck Foundation and the MIND Institute. The General Clinical Research Center was supported by NIH grant M01-RR00400.

References

- [1] Ugurbil K, Brown TR, Den Hollander JA, Glynn P, Shulman RG. High-resolution ^{13}C nuclear magnetic resonance studies of glucose metabolism in *Escherichia coli*. Proc Natl Acad Sci U S A 1978; 75(8):3742–6.
- [2] Den Hollander JA, Brown TR, Ugurbil K, Shulman RG. ^{13}C Nuclear magnetic resonance studies of anaerobic glycolysis in suspensions of yeast cells. Proc Natl Acad Sci U S A 1979;76(12):6096–100.
- [3] Chance MC, Seeholzer SH, Kobayashi K, Williamson JR. Mathematical analysis of isotope labeling in the citric acid cycle with applications to ^{13}C NMR studies in perfused rat hearts. J Biol Chem 1983;258:13785–94.
- [4] Rothman DL, Behar KL, Hetherington HP, den Hollander JA, Bendall MR, Petroff OAC, et al. ^1H -Observe/ ^{13}C -decouple spectroscopic measurements of lactate and glutamate in the rat brain in vivo. Proc Natl Acad Sci U S A 1985;82:1633–7.
- [5] Behar KL, Petroff OAC, Prichard JW, Alger JR, Shulman RG. Detection of metabolites in rabbit brain by ^{13}C NMR spectroscopy following administration of $[1-^{13}\text{C}]\text{glucose}$. Magn Reson Med 1986; 3:911–20.
- [6] Mason GF, Rothman DL, Behar KL, Shulman RG. NMR determination of the TCA cycle rate and α -ketoglutarate/glutamate exchange rate in rat brain. J Cereb Blood Flow Metab 1992;12:434–47.
- [7] Gruetter R, Novotny EJ, Boulware SD, Mason GF, Rothman DL, Shulman GI, et al. Localized ^{13}C NMR spectroscopy in the human brain of amino acid labeling from D- $[1-^{13}\text{C}]\text{glucose}$. J Neurochem 1994;63:1377–85.
- [8] Sibson NR, Dhankhar A, Mason GF, Behar KL, Rothman DL, Shulman RG. In vivo ^{13}C NMR measurements of cerebral glutamine synthesis as evidence for glutamate–glutamine cycling. Proc Natl Acad Sci U S A 1997;94:2699–704.
- [9] Garcia-Espinosa MA, Rodrigues TB, Sierra A, Benito M, Fonseca C, Gray HL, et al. Cerebral glucose metabolism and the glutamine cycle as detected by in vivo and in vitro ^{13}C NMR spectroscopy. Neurochem Int 2004;45(2–3):297–303.
- [10] Hyder F, Rothman DL, Mason GF, Rangarajan A, Behar KL, Shulman RG. Oxidative glucose metabolism in rat brain during single forepaw stimulation: a spatially localized $^1\text{H}\{^{13}\text{C}\}$ nuclear magnetic resonance study. J Cereb Blood Flow Metab 1997;17:1040–7.
- [11] Chen W, Zhu XH, Gruetter R, Seaquist ER, Adriany G, Ugurbil K. Study of tricarboxylic acid cycle flux changes in human visual cortex during hemifield visual stimulation using $^1\text{H}\{^{13}\text{C}\}$ MRS and fMRI. Magn Reson Med 2001;45(3):349–55.
- [12] Chhina N, Kuestermann E, Halliday J, Simpson LJ, Macdonald IA, Bachelard HS, et al. Measurement of human tricarboxylic acid cycle rates during visual activation by ^{13}C magnetic resonance spectroscopy. J Neurosci Res 2001;66(5):737–46.
- [13] Gruetter R, Seaquist ER, Ugurbil K. A mathematical model of compartmentalized neurotransmitter metabolism in the human brain. Am J Physiol 2001;281:E100–12.
- [14] Oz G, Berkich DA, Henry PG, Xu Y, LaNoue K, Hutson SM, et al. Neuroglial metabolism in the awake rat brain: CO_2 fixation increases with brain activity. J Neurosci 2004;24(50):11273–9.
- [15] Gruetter R, Adriany G, Choi I-Y, Henry P-G, Lei H-X, Oz G. Localized in vivo ^{13}C NMR spectroscopy of the brain. NMR Biomed 2003;16:313–38.

- [16] de Graaf RA, Mason GF, Patel AB, Behar KL, Rothman DL. In vivo ^1H - ^{13}C -NMR spectroscopy of cerebral metabolism. *NMR Biomed* 2003;16(6–7):339–57.
- [17] Sibson NR, Mason GF, Shen J, Cline GW, Herskovits AZ, Wall JE, et al. In vivo ^{13}C NMR measurement of neurotransmitter glutamate cycling, anaplerosis and TCA cycle flux in rat brain during $[2\text{-}^{13}\text{C}]\text{glucose}$ infusion. *J Neurochem* 2001;76(4):975–89.
- [18] Cerdan S, Kunnecke B, Seelig J. Cerebral metabolism of $[1,2\text{-}^{13}\text{C}]\text{acetate}$ as detected by in vivo and in vitro ^{13}C NMR. *J Biol Chem* 1990;265(22):12916–26.
- [19] Lebon V, Petersen KF, Cline GW, Shen J, Mason GF, Dufour S, et al. Astroglial contribution to brain energy metabolism in humans revealed by ^{13}C nuclear magnetic resonance spectroscopy: elucidation of the dominant pathway for neurotransmitter glutamate repletion and measurement of astrocytic oxidative metabolism. *J Neurosci* 2002;22(5):1523–31.
- [20] Pan JW, de Graaf RA, Petersen KF, Shulman GI, Hetherington HP, Rothman DL. $[2,4\text{-}^{13}\text{C}]\text{-}\beta\text{-hydroxybutyrate}$ metabolism in human brain. *J Cereb Blood Flow Metab* 2002;22(7):890–8.
- [21] Ross B, Lin A, Harris K, Bhattacharya P, Schweinsburg B. Clinical experience with ^{13}C MRS in vivo. *NMR Biomed* 2003;16(6–7):358–69.
- [22] Mason GF, Falk Petersen K, de Graaf RA, Kanamatsu T, Otsuki T, Rothman DL. A comparison of ^{13}C NMR measurements of the rates of glutamine synthesis and the tricarboxylic acid cycle during oral and intravenous administration of $[1\text{-}^{13}\text{C}]\text{glucose}$. *Brain Res Protoc* 2003;10(3):181–90.
- [23] Duckrow RB, Bryan Jr RM. Regional cerebral glucose utilization during hyperglycemia. *J Neurochem* 1987;48(3):989–93.
- [24] Gruetter R, Adriany G, Merkle H, Andersen PM. Broadband decoupled, ^1H -localized ^{13}C MRS of the human brain at 4 Tesla. *Magn Reson Med* 1996;36:659–64.
- [25] Henry P-G, Tkac I, Gruetter R. ^1H -Localized broadband ^{13}C NMR spectroscopy of the rat brain in vivo at 9.4 Tesla. *Magn Reson Med* 2003;50(4):684–92.
- [26] Marjanska M, Henry P-G, Gruetter R, Garwood M, Ugurbil K. A new method for proton detected carbon edited spectroscopy using LASER. 12th ed. Kyoto (Japan): ISMRM; 2004. p. 679.
- [27] Beckmann N, Turkalj I, Seelig J, Keller U. ^{13}C NMR for the assessment of human brain glucose metabolism in vivo. *Biochemistry* 1991;30(30):6362–6.
- [28] Gruetter R, Rothman DL, Novotny EJ, Shulman RG. Localized ^{13}C NMR spectroscopy of *myo*-inositol in the human brain in vivo. *Magn Reson Med* 1992;25(1):204–10.
- [29] Gruetter R, Seaquist ER, Kim S, Ugurbil K. Localized in vivo ^{13}C -NMR of glutamate metabolism in the human brain: initial results at 4 Tesla. *Dev Neurosci* 1998;20:380–8.
- [30] Henry P-G, Oz G, Provencher S, Gruetter R. Toward dynamic isotopomer analysis in the rat brain in vivo: automatic quantitation of ^{13}C NMR spectra using LCModel. *NMR Biomed* 2003;16:400–12.
- [31] Rothman DL, Novotny EJ, Shulman GI, Howseman AM, Petroff OAC, Mason G, et al. ^1H - ^{13}C NMR measurements of $[4\text{-}^{13}\text{C}]\text{glutamate}$ turnover in human brain. *Proc Natl Acad Sci U S A* 1992;89:9603–6.
- [32] Mason GF, Pan JW, Chu W-J, Newcomer BR, Zhang Y, Orr R, et al. Measurement of the tricarboxylic acid cycle rate in human grey and white matter in vivo by ^1H - ^{13}C magnetic resonance spectroscopy at 4.1T. *J Cereb Blood Flow Metab* 1999;19:1179–88.
- [33] Henry P-G, Roussel R, Vaufrey F, Dautry C, Bloch G. Semiselective POCE NMR spectroscopy. *Magn Reson Med* 2000;44(3):395–400.
- [34] Pfeuffer J, Tkac I, Choi I-Y, Merkle H, Ugurbil K, Garwood M, et al. Localized in vivo ^1H NMR detection of neurotransmitter labeling in rat brain during infusion of $[1\text{-}^{13}\text{C}]\text{D-glucose}$. *Magn Reson Med* 1999;41:1077–83.
- [35] De Graaf RA, Brown PB, Mason GF, Rothman DL, Behar KL. Detection of $[1,6\text{-}^{13}\text{C}]\text{-glucose}$ metabolism in rat brain by in vivo ^1H - ^{13}C -NMR spectroscopy. *Magn Reson Med* 2003;49(1):37–46.
- [36] Henry P-G, Marjanska M, Gruetter R, Ugurbil K. Effect of strong scalar coupling in proton-observed carbon-edited NMR spectroscopy. 13th ISMRM, Miami (FL), 2005. p. 57.
- [37] Yahya A, Allen PS. 3D localized direct ^{13}C detection using PRESS and a modified DEPT sequence. 13th ISMRM, Miami (FL), 2005. p. 344.
- [38] Henry PG, Lebon V, Vaufrey F, Brouillet E, Hantraye P, Bloch G. Decreased TCA cycle rate in the rat brain after acute 3-NP treatment measured by in vivo ^1H - ^{13}C NMR spectroscopy. *J Neurochem* 2002;82(4):857–66.
- [39] Mason GF, Rothman DL. Basic principles of metabolic modeling of NMR ^{13}C isotopic turnover to determine rates of brain metabolism in vivo. *Metab Eng* 2004;6(1):75–84.
- [40] Mason GF, Gruetter R, Rothman DL, Behar KL, Shulman RG, Novotny EJ. Simultaneous determination of the rates of the TCA cycle, glucose utilization, α -ketoglutarate/glutamate exchange, and glutamine synthesis in human brain by NMR. *J Cereb Blood Flow Metab* 1995;15:12–25.
- [41] Choi IY, Lei HX, Gruetter R. Effect of deep pentobarbital anesthesia on neurotransmitter metabolism in vivo: on the correlation of total glucose consumption with glutamatergic action. *J Cereb Blood Flow Metab* 2002;22(11):1343–51.
- [42] Yu X, Alpert NM, Lewandowski ED. Modeling enrichment kinetics from dynamic ^{13}C -NMR spectra: theoretical analysis and practical considerations. *Am J Physiol* 1997;272(6 Pt 1):C2037–48.
- [43] Berkich DA, Xu Y, LaNoue KF, Gruetter R, Hutson SM. Evaluation of brain mitochondrial glutamate and α -ketoglutarate transport under physiologic conditions. *J Neurosci Res* 2005;79(1–2):106–13.
- [44] Sibson NR, Dhankhar A, Mason GF, Rothman DL, Behar KL, Shulman RG. Stoichiometric coupling of brain metabolism and glutamatergic neuronal activity. *Proc Natl Acad Sci U S A* 1998;95:316–21.
- [45] Shen J, Petersen KF, Behar KL, Brown P, Nixon TW, Mason GF, et al. Determination of the rate of the glutamate/glutamine cycle in the human brain by in vivo ^{13}C NMR. *Proc Natl Acad Sci U S A* 1999;96:8235–40.
- [46] Patel AB, de Graaf RA, Mason GF, Rothman DL, Shulman RG, Behar KL. The contribution of GABA to glutamate/glutamine cycling and energy metabolism in the rat cortex in vivo. *Proc Natl Acad Sci U S A* 2005;102(15):5588–93.
- [47] Boumezbeur F, Besret L, Valette J, Vaufrey F, Henry PG, Slavov V, et al. NMR measurement of brain oxidative metabolism in monkeys using ^{13}C -labeled glucose without a ^{13}C radiofrequency channel. *Magn Reson Med* 2004;52(1):33–40.
- [48] Boumezbeur F, Besret L, Valette J, Gregoire MC, Delzescaux T, Maroy R, et al. Glycolysis versus TCA cycle in the primate brain as measured by combining $(18)\text{F-FDG}$ PET and ^{13}C -NMR. *J Cereb Blood Flow Metab* 2005;25(11):1418–23.
- [49] Deelchand DK, Ugurbil K, Henry P-G. Investigating brain metabolism at high fields using localized ^{13}C NMR spectroscopy without ^1H decoupling. *Magn Reson Med* 2006;55:279–86.